

7.6. Barrow, Alaska

UV radiation at Barrow differs from that at austral high latitude sites in several ways. For example, the “ozone-sensitive” data products, particularly biologically effective dose-rates and the integral around 300 nm, show much smaller short-term variability than at the austral sites due to less severe ozone depletion in the Arctic.

In Figure 7.6.1, recent column ozone data from the Ozone Monitoring Instrument (OMI) onboard NASA’s AURA satellite are compared with ozone records from the years 1991-2013. There is a strong seasonal dependence: ozone columns are generally higher and have a larger variability during spring than autumn. After a large drop in total ozone on 23 March 2014, total ozone was above average between 26 March and 11 April 2014. Between mid-April and the end of September, ozone measurements in 2014 varied about the average calculated from measurements of the year 1991 – 2013. Total ozone was unusually large during October 2014.

The daily maximum UV Index (Figure 7.6.2) was somewhat suppressed between the beginning of May and end of June 2014 compared to historical measurements. This may have two reasons: relative low surface albedo between mid-April and the end of May (ranging from 0.6 to 0.8 in 2014 instead of the more typical range of 0.8 to 0.9) and higher-than-normal cloudiness. Relatively low UV values during this period were also observed for other data products such as the spectral irradiance integrated over 298.51 - 303.03 nm (Figure 7.6.3), DNA-weighted daily dose (Figure 7.6.4), and erythemally-weighted daily dose (Figure 7.6.5), respectively.

Daily irradiation in the 400-600 nm band is shown in Figure 7.6.6. Visible radiation is virtually not affected by the ozone column and changes in surface albedo have a smaller effect compared to wavelengths in the UV. Measurements up to the end of April 2014 agree reasonably well with historical data. However, also data in the visible are unusually low between 9 and 23 May 2014 and during the first half of June. Higher-than-normal cloudiness is the likely reason. In general, radiation levels at all wavelengths are much more affected by clouds during summer and autumn than during spring because high albedo in spring resulting from snow cover reduces cloud effects.

Factors affecting the annual cycles in UV and visible radiation at Barrow have been analyzed in great detail (Bernhard *et al.*, 2007). The annual ozone cycle was found to be the dominant parameter modifying UV-B irradiance, but the combined effects of albedo and clouds compensate for most of the ozone influence. High surface albedo caused by snow cover may increase UV irradiance by up to 57%. Aerosols lead to reductions of 5% typically, but larger reduction may be observed during Arctic haze events, particularly during spring. For erythema irradiance, and measurements in the UV-A and visible, annual cycles of albedo and clouds are responsible for a pronounced seasonal asymmetry.

An example of the different characteristics of DNA-damaging and visible radiation is shown in Figure 7.6.7. Daily irradiation in the 400-600 nm spectral range is not centered at the summer solstice but shifted by about 15 days towards spring. DNA-damaging radiation on the other hand is nearly symmetrical with respect to the solstice. The reason for this distinct difference can be explained as follows: surface albedo is larger and clouds are less prevalent in spring than in autumn. This enhances radiation levels in spring and is the reason of the apparent shift of measurements in the visible range. Higher albedo and less cloudiness also leads to larger DNA-damaging radiation, but the larger total ozone column in spring (Figure 7.6.1) compensates the enhancement. As a consequence, DNA-damaging radiation is of similar magnitude in spring and autumn.

Reference:

Bernhard, G., C. R. Booth, J. C. Ehamjian, R. Stone, and E. G. Dutton (2007), Ultraviolet and visible radiation at Barrow, Alaska: Climatology and influencing factors on the basis of version 2 National Science Foundation network data, *J. Geophys. Res.*, 112, D09101, doi:10.1029/2006JD007865.

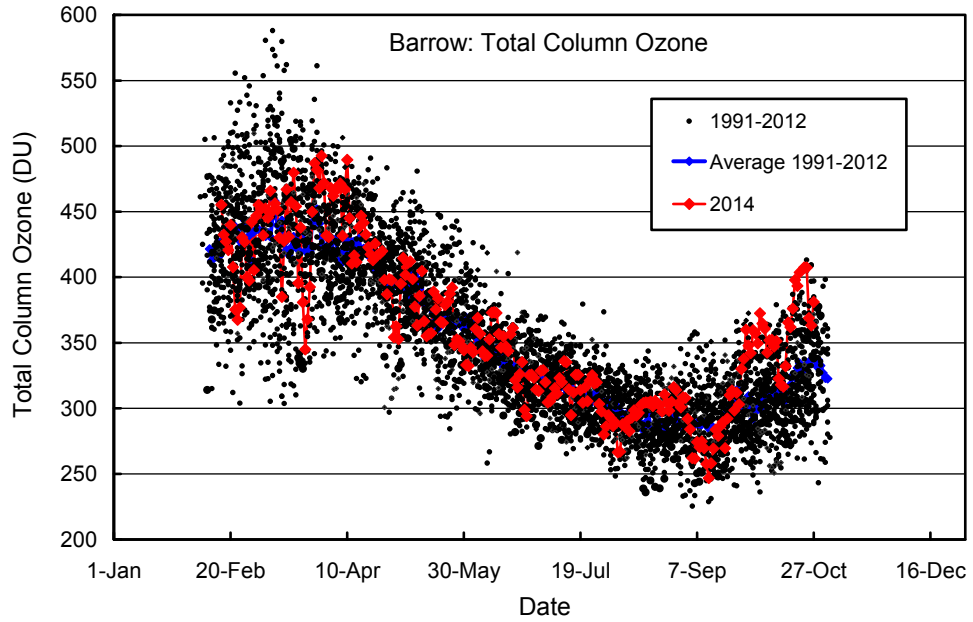


Figure 7.6.1. Total column ozone at Barrow. OMI measurements from 2014 are contrasted with ozone satellite data from prior years recorded by TOMS/Nimbus-7 (1991-1993), TOMS/Earth Probe (1996-2004), and OMI (2005-2013). TOMS data are from the Version 8 data set.

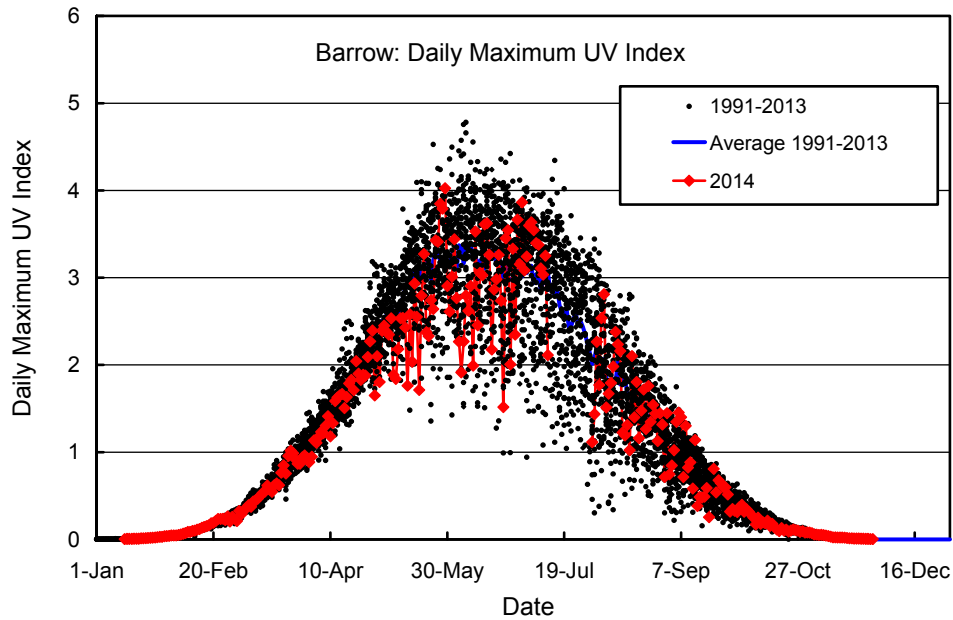


Figure 7.6.2. Daily maximum UV Index at Barrow. Measurements from 2014 are contrasted with individual data points and the average of measurements taken between 1991 and 2013.

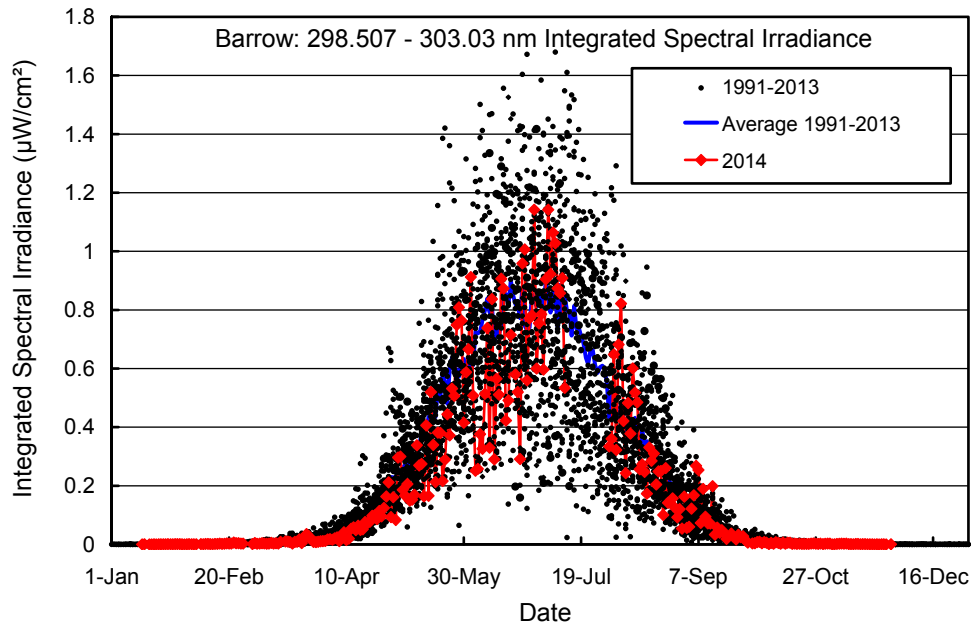


Figure 7.6.3. Noontime integrated spectral UV irradiance (298.51 - 303.03 nm) at Barrow. Measurements from 2014 are contrasted with individual data points and the average of measurements taken between 1991 and 2013.

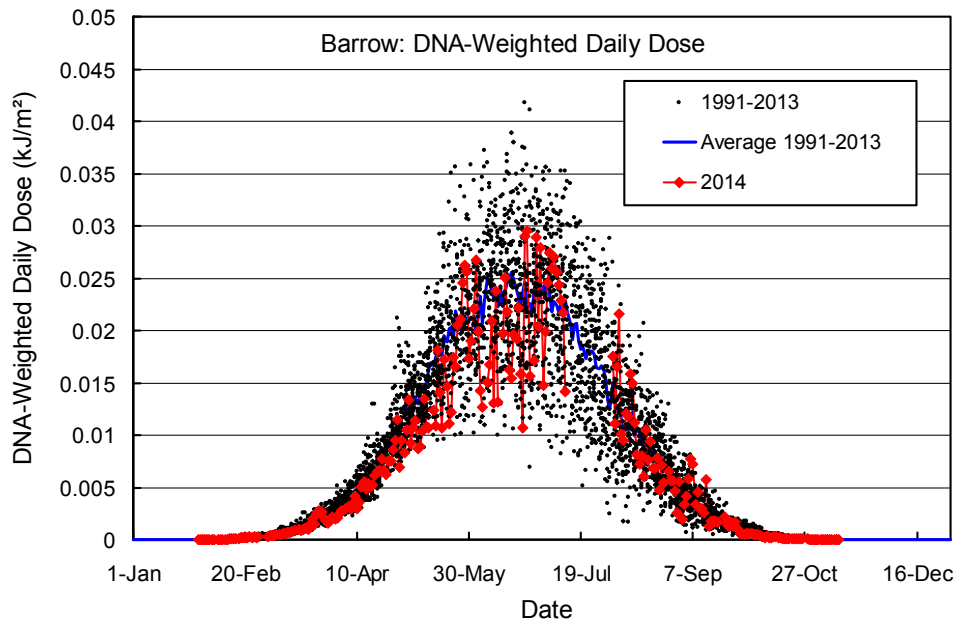


Figure 7.6.4. Daily DNA-weighted dose at Barrow. Volume 24 measurements from 2014 are contrasted with individual data points and the average of measurements taken between 1991 and 2013.

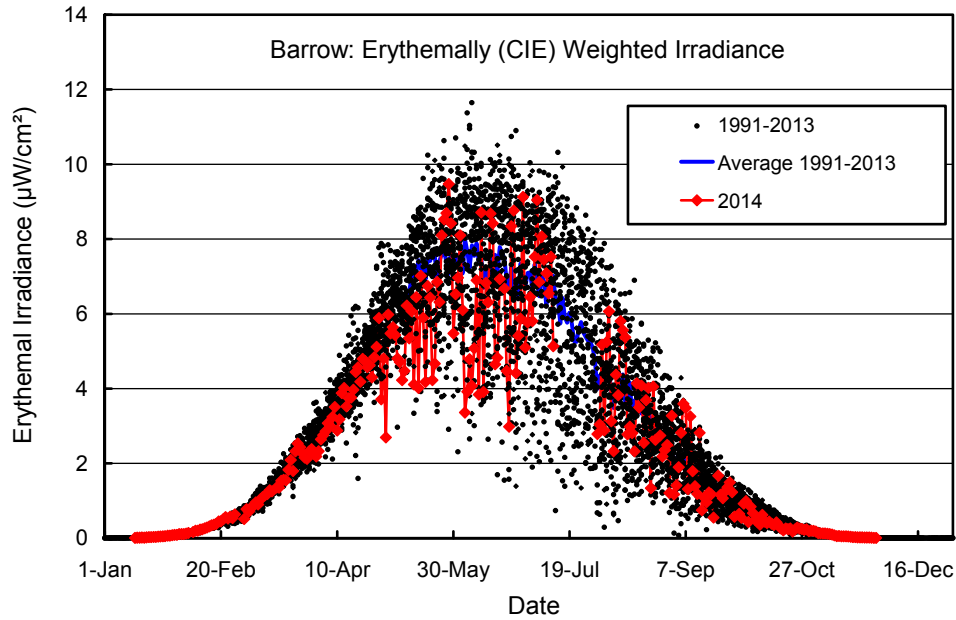


Figure 7.6.5. Daily erythemal dose at Barrow. Volume 24 measurements from 2014 are contrasted with individual data points and the average of measurements taken between 1991 and 2013.

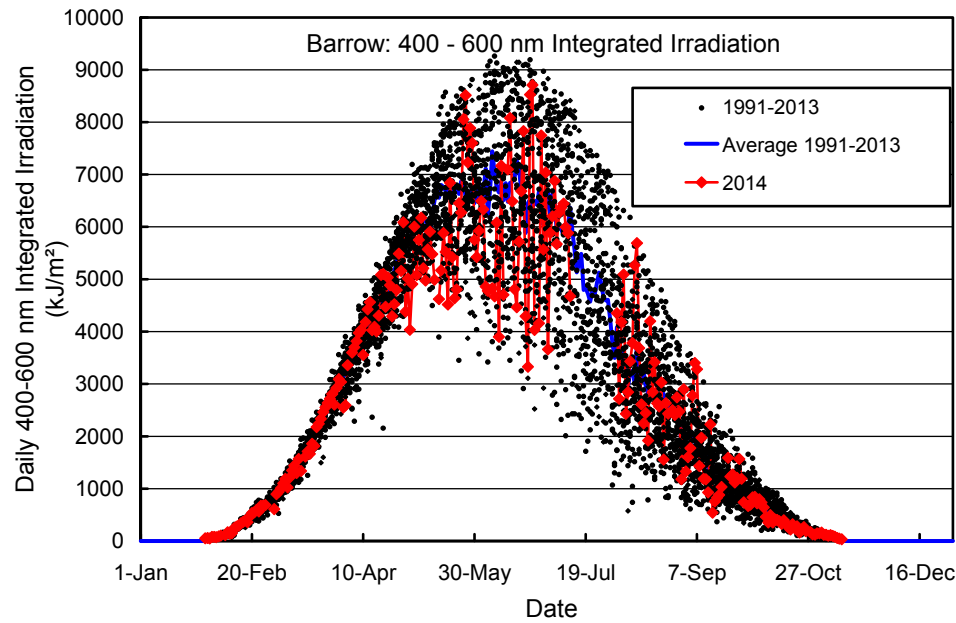


Figure 7.6.6. Daily irradiation of the 400-600 nm band at Barrow. Volume 24 measurements from 2014 are contrasted with individual data points and the average of measurements taken between 1991 and 2013.

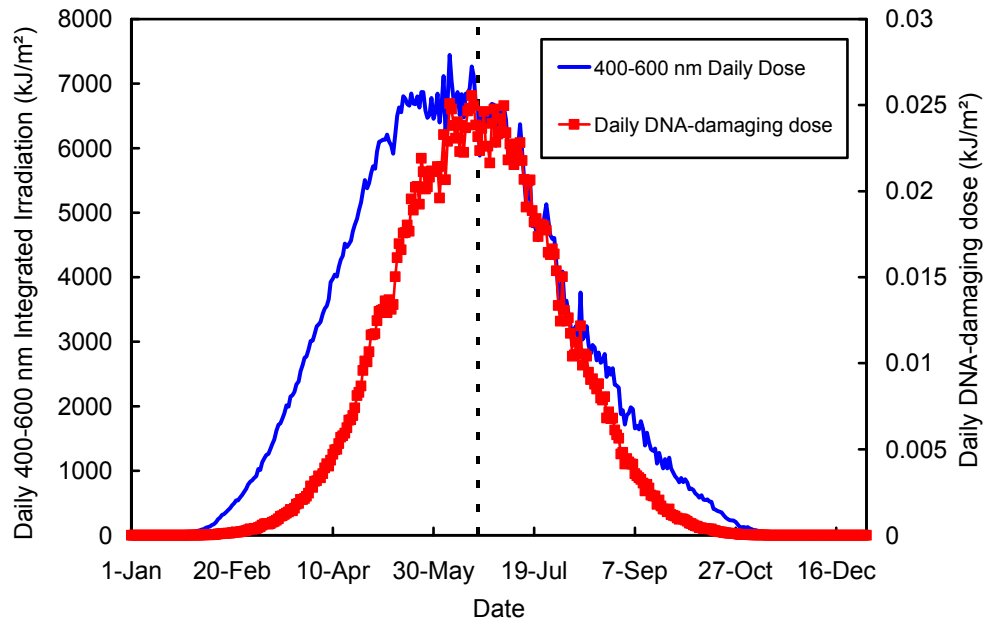


Figure 7.6.7. Comparison of DNA-weighted dose (right axis) with daily irradiation in the 400-600 nm spectral range (left axis) at Barrow. Both curves are average values for the period 1991-2013. The broken line indicates the summer solstice.